

# Solid-Liquid Mass Transfer in Packed Beds with Cocurrent Gas-Liquid Downflow

Local instantaneous solid-liquid mass transfer coefficients were measured in two-phase gas-liquid downflow through packed columns for  $3 \times 3$  mm and  $6 \times 6$  mm cylinders. An electrochemical technique was used. Liquid flow rates from 3.0 to 26.6 kg/m<sup>2</sup>s and gas flow rates from 0.07 to 1.16 kg/m<sup>2</sup>s covered the gas-continuous, ripple, and pulse flow regimes. Time-averaged mass transfer coefficients in trickle flow and in pulse flow for the pulse proper and the base (outside the pulse) were found to increase with increasing gas and liquid rates. Correlations are presented in terms of liquid phase Reynolds numbers and in terms of Kolmogoroff numbers. The mass transfer coefficients in the pulse were found to correspond closely to the coefficients that would be attained in the dispersed bubble flow regime.

V. G. RAO and

A. A. H. DRINKENBURG

Department of Chemical Engineering  
Rijksuniversiteit Groningen  
9747 AG Groningen, The Netherlands

## SCOPE

Trickle-bed reactors, when operated in the gas-continuous trickle flow regime, are generally restricted to relatively slow reactions since the rate is often controlled by the mass transfer resistance. Operation of the reactor at higher gas and liquid rates produces pulse flow in which high transfer rates can be realized (Hirose et al., 1976). The pulse flow regime is better suited for fast reactions than the trickle flow regime. For design, the resistance to absorption of gaseous components into the liquid and the transfer of the reacting species through the liquid film to the catalyst surface must be known, which necessitates the study of solid-liquid mass transfer. The many reported studies on solid-liquid mass transfer generally have utilized one of two methods: measuring the dissolution rate of some soluble packing or packing coated with a soluble dye, or measuring the electrical current in water under diffusion-limited transport conditions.

The electrochemical method has certain advantages over the other. It facilitates direct and instantaneous measurements of solid-liquid mass transfer and is thus very useful to measure mass transfer fluctuations, especially under pulsing flow conditions. Chou et al. (1979) first measured such fluctuations in pulse flow. The pulses were found to play an important role in enhancing mass transfer coefficients. Not much is known about

the mass transfer coefficients in the pulses, their dependence on flow rate of the phases, and the packing properties. No study other than Chou's has been reported in this direction. All earlier studies employed the dissolution method, from which only time-averaged values were found.

The present study was conducted to understand the fundamental nature of the pulses with respect to mass transfer, the extent of mass transfer fluctuations, and their qualitative and quantitative influence on mass transfer. The instantaneous mass transfer from a single active particle (brass cylinder electrochemically coated with nickel) in the bed was measured. Beds with particles of  $3 \times 3$  mm and  $6 \times 6$  mm cylinders were used. The active particle had the same dimensions as the bed material. Time-averaged mass transfer for the pulse proper and base (outside the pulse) were computed. The electrolytic solution was a mixture of approximately 0.006 M potassium ferriyanide, 0.05 M potassium ferrocyanide, and a large excess of approximately 1 M sodium hydroxide as a supporting electrolyte. Air was the gaseous phase. A wide range of flow rates was covered to realize trickle, ripple, and pulse flow regimes. Liquid flow rates were varied from 3.0 to 26.6 kg/m<sup>2</sup>s. Gas rates were varied from 0.07 to 1.16 kg/m<sup>2</sup>s.

## CONCLUSIONS AND SIGNIFICANCE

The electrochemical method measures the product of the local instantaneous mass transfer rate and fractional surface wetting,  $\phi$ . Results were obtained in trickle, ripple, and pulse flow regimes in terms of  $\phi k_s$ , where  $k_s$  is the solid-liquid mass transfer coefficient. For comparison and correlation of the results,  $k_s$

is expressed in a Sherwood number,  $Sh$ . The nature of the flow regime has a very significant influence on mass transfer rates; a steep increase of mass transfer occurs in the ripple flow regime, the transition from trickle flow to pulse flow. The Sherwood number increases with increasing gas and liquid rates in all flow regimes. The mass transfer fluctuations in pulse flow were very large. The pulse mass transfer was higher by about 2.5 to 3.5 times over the base mass transfer parts outside the

V. G. Rao is currently at the Department of Chemical Engineering, Indian Institute of Technology, Bombay 400 076, India.  
Present address of A. A. H. Drinkenburg: DSM-Research, 6160 MD Geleen, the Netherlands.

pulse. A typical comparison at  $L = 7.86 \text{ kg/m}^2\text{s}$  for 6 mm cylinders indicated that  $\phi Sh$  for base, average, and pulse increased by about 2, 3, and 5.5 times, respectively, to  $\phi Sh$  in trickle flow at the transition.  $\phi k_s$  was found to increase with a decrease of particle diameter from 6 mm cylinders to 3 mm cylinders. The mass transfer enhancement due to decreasing particle diameter is about 40% in the pulses (high interaction between the phases) and about 17% for base mass transfer (low interaction regime).

The proposed correlation in terms of the Reynolds number in pulse flow correlates the data of earlier studies within 20% error bounds for cylinders, spheres, and Berl saddles from 2.8 to 12.7 mm dia., for a range of liquid rates from 7.5 to 95  $\text{kg/m}^2\text{s}$ ,

and for a range of gas rates from 0.08 to 2.4  $\text{kg/m}^2\text{s}$ . The average mass transfer in pulse flow, when correlated in terms of the Kolmogoroff number, was not influenced explicitly by the particle diameter, although the particle diameter was found to have an explicit effect on the pulse mass transfer rates. The pulse mass transfer coefficients were found to correspond to the coefficients that would be obtained in the dispersed bubble flow regime. This finding together with the knowledge of bubble dispersion in the pulse, observed in our laboratory by high speed photography, indicates that the hydrodynamic mechanism that exists in the pulses closely corresponds to that in dispersed bubble flow.

## INTRODUCTION

Two-phase gas-liquid downflow through packed beds, often called trickle beds, finds extensive use in the petroleum industry and in oxidation processes, for example, oxidation of dissolved organic pollutants in industrial wastewater. Interphase mass transfer—mass transfer from gas to liquid and liquid to solid—often controls the performance of these reactors. Solid-liquid mass transfer resistance is significant when the following inequality is satisfied (Satterfield, 1975):

$$(10d_p/c)r(1-\epsilon) > K_{LS} \quad (1)$$

Hence for highly active catalysts or fast reactions and/or relatively large catalyst particles, the liquid film becomes the controlling resistance.

Following the initial study by Van Krevelen and Krekels (1948), there have been several investigations on solid-liquid mass transfer (Table 1). Generally either dissolution of slightly soluble packing into the liquid or electrochemical reactions were used for the measurements. The electrochemical technique gives the instantaneous mass transfer coefficients by measuring the limiting current under diffusion-limited transport conditions at relatively high voltage. Then the current is independent of the potential at the working electrode and is a direct measure of the diffusive flux. The method is well suited to study fluctuations in mass transfer, for example, in pulse flow.

Pulse flow is characterized by high density (liquid-rich) and low density (gas-rich) mixtures flowing successively through the bed, causing a high level of turbulence. The regime is encountered at intermediate gas and liquid rates, bordered on one side by gas-continuous trickle and ripple flow at lower liquid rates and on the other side by dispersed bubble flow at higher liquid rates. The low density part outside the pulse is more like trickle flow; the high density part in the pulse resembles dispersed bubble flow. The objective of this study was to characterize the solid-liquid mass transfer coefficients in and outside the pulses.

## EXPERIMENTAL

### Apparatus and Procedure

A diagram of the experimental apparatus is shown in Figure 1. The trickle-bed column was made of glass having an I.D. of 5 cm. The column was packed with 3 × 3 mm or 6 × 6 mm glass cylinders. Air and liquid were fed at the top of the column (1). The liquid was distributed over the packing by means of three tubes, and the air entered the column flow behind through the distributor head (2). Air and liquid flow rates were measured by a set of rotameters (4). The flow rates were held constant by means of

flowstats (5) irrespective of the column pressure drop variations.

The air was saturated with water in a humidification column (3) packed with Berl saddles before entering the main column. Water was fed to the humidification column countercurrently with the air.

Two pressure taps (10) were provided, one just above the packing at the top through the distributor head and the other through a supporting grid of the packing at the bottom of the column. The pressure drop in the column was measured using either a mercury or a water U-tube manometer (11), depending on the flow rates of the phases.

Instantaneous solid-liquid mass transfer for a single particle in the bed was determined under diffusion-limited transport conditions at the working electrode. For this purpose the column was divided into different packed sections, having a total length of 240 cm. A test section 30 cm long was kept between entrance and exit sections of 100 and 110 cm, length respectively.

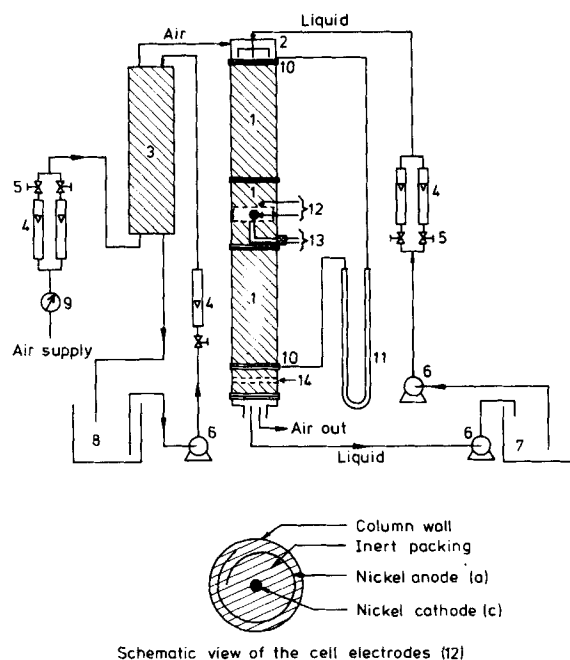


Figure 1. Experimental apparatus.

- |                            |                                       |
|----------------------------|---------------------------------------|
| (1) Packed sections.       | (8) Water tank.                       |
| (2) Liquid distributor.    | (9) Pressure regulator.               |
| (3) Humidification column. | (10) Pressure taps.                   |
| (4) Rotameters.            | (11) Manometer.                       |
| (5) Flowstats.             | (12) Electrochemical cell electrodes. |
| (6) Pumps.                 | (13) Lead wires.                      |
| (7) Liquid tank.           | (14) Copper mesh electrodes.          |

TABLE 1. SUMMARY OF PREVIOUS RELEVANT STUDIES

Author	Packing Size and Shape	Packing Material	Gas and Liquid Phases	$G$ kg/m <sup>2</sup> -s	$L$ kg/m <sup>3</sup> -s	Correlation
Lemay et al. (1975) Goto et al. (1975)	6.25 mm spheres 2.4 mm granular 0.54, 1.08 and 2.4 mm granular 3.17 × 3.17 mm cylinders	Benzoic acid -naphthol Naphthalene Benzoic acid	Air-water Air-water Air-water Air-water	0.37-0.9 0-0.009 0-0.009 0.23-0.93	13-40 0.48-5.2 0.48-5.2 3.5-19.7	Pulse flow: $k_g Sc^{2/3} = 0.20 (E'_{\mu L} / \rho_L)^{0.25}$ Trickle flow: Graphical correlation in terms of $j_D$ and $Re_L$ $k_g = 1.305 [L^{-0.78} \{1 - (e^y/1 + e^y)\}]^{0.38} G^{0.38}$ $y = 4L/6350, L, G$ in lb <sub>m</sub> /ft <sup>2</sup> -h, $k_g$ in ft/s
Sylvester and Pitaagalsarn (1975)	2.8, 5.5, 12 mm spheres 3.2, 6.4, 12.7 mm spheres	Benzoic acid Brass	Nitrogen(?) -water Nitrogen(?) -potassium dichromate in aqueous sulfuric acid	0.2-2.3 0-1.9	0.53-245 1.6-8.3	Single-phase flow: $Sh/Sc^{1/3} = 0.80 Re_L^{0.5} 20 < 200$ $Sh/Sc^{1/3} = 0.53 Re_L^{0.58} 200 < Re_L < 5000$ Pulse and dispersed bubble flow: In terms of an enhancement factor as compared to single phase flow Trickle flow ( $G = 0$ ) $Sh''/Sc^{1/3} = 2.79 (Re_L)^{0.70}$ Gas-continuous and pulse flow: $\ln (Sh''/Sc^{1/3}) = 1.84 + 0.311 \ln(ue \times 10^3) - 6.33/\ln(ue \times 10^3)^2$
Specchia et al. (1978)	3 × 3 mm cylinders 6 × 6 mm cylinders	Benzoic acid	Air-water, water + surfactants, water + glycerol	0-1.9	1.6-8.3	Trickle flow ( $G = 0$ ) $Sh''/Sc^{1/3} = 0.815 Re_L^{0.822}, Re_L'' \leq 60$ Pulse flow: $Sh''/Sc^{1/3} = 0.334 Ko^{0.202}$
Satterfield et al. (1978)	3 × 3, 6 × 6 mm cylinders	Benzoic acid	Nitrogen, helium argon-water	0-1.6	0.5-25	Trickle flow ( $G = 0$ ) $Sh''/Sc^{1/3} = 0.815 Re_L^{0.822}, Re_L'' \leq 60$ Pulse flow: $Sh''/Sc^{1/3} = 0.334 Ko^{0.202}$
Chou et al. (1979)	7.8 mm spheres	Nickel (electrochemical reaction)	Air-potassium ferri and ferrocyanides in sodium hydroxide	0.09-0.69	7.2-20	Gas-continuous flow: $Re_L^* < 55$ $Sh''/Sc^{1/3} = 0.0819 (Re_L^*)^{0.777}$ Transition: $55 < Re_L^* < 100$ $Sh''/Sc^{1/3} = 0.00437 (Re_L^*)^{1.517}$ Pulse and dispersed bubble flow: $Re_L^* > 100$ $Sh''/Sc^{1/3} = 0.68 (Re_L^*)^{0.416}$ $Sh''/Sc^{1/3} = 0.43 Ko^{0.22}$
Ruether et al. (1980)	6.35 mm Berl saddles	Benzoic acid + rhodamine	Air-water	0.33-1.77	2.1-94.4	
DeLaunay et al. (1982)	4 mm spheres	Nickel (electrochemical reaction)	Nitrogen-potassium ferri and ferrocyanides in sodium hydroxide	0.01-0.4	0.5-5	

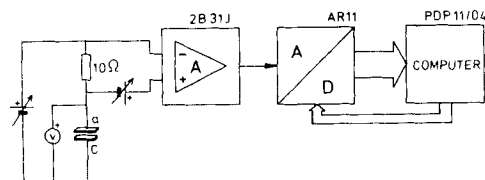


Figure 2. A schematic of mass transfer acquisition system: A, amplifier; A/D, analog-digital converter; a, anode; c, cathode.

The long entrance and exit sections were preferred to eliminate the end effects observed by Chou et al. (1979).

The cathode was either a 3 × 3 mm or a 6 × 6 cm cylinder depending on the inert packing material and was made of brass electrochemically coated with nickel. A thin nickel foil having a large surface area (2.5 × 15 cm) was used as the anode to prevent polarization of the anode. The cathode was always placed at the center of the column about 15 cm below the top of the test section. The nickel anode was placed in a spiral shape next to the wall of the column separated through a layer of the inert packing particles, as shown in the detail of the cell electrodes (12) in Figure 1. In this type of configuration electrolytic flow is perpendicular to the electric current. The configuration was first used by Delaunay et al. (1980) in upward cocurrent gas-liquid flow in packed beds. The crossflow configuration was chosen for two reasons: Besides providing a better potential distribution in the solution, it greatly reduces the ohmic potential drop between the electrodes, especially at low liquid holdup levels, thus favoring a wider limiting current plateau. The electrodes were frequently cleaned by dipping them into dilute hydrochloric acid. Whenever the electrodes were cleaned, a portion of the packing material from the test section had to be taken out and care was taken to refill it with the same amount of packing material.

The electrolytic solution was a mixture of approximately 0.006 M potassium ferricyanide, 0.05 M potassium ferrocyanide, and a large excess of approximately 1 M sodium hydroxide as a supporting electrolyte. The supporting electrolyte reduces the migration effect. Initial trials with commercial grade potassium ferri- and ferrocyanides indicated decomposition of the solution within a week or less. In view of this, analytical grade ferri- and ferrocyanides were used, which improved the use of the solution for a longer time. However, no solution was used more than four days. The concentration of potassium ferricyanide was measured before each experiment.

Pulse frequencies were measured with the help of two copper mesh electrodes (14) placed between the packing about 5 cm above from the bottom of the column. Additional details of this method can be found elsewhere (Blok and Drinkenburg, 1982). All the experiments were done

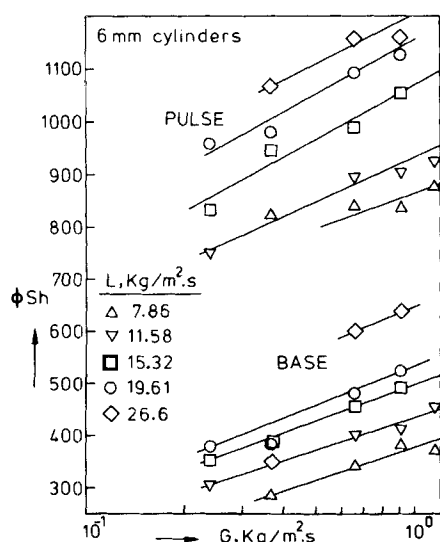


Figure 3. Experimental pulse and base mass transfer as a function of gas mass velocity, 6 mm cylinders.

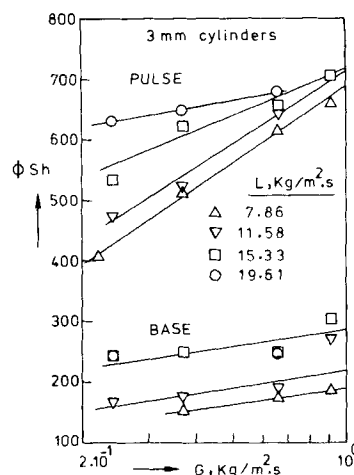


Figure 4. Experimental pulse and base mass transfer as a function of gas mass velocity, 3 mm cylinders.

at 20°C. The diffusivity of ferricyanide was calculated from the equation given by Hiraoka et al. (1981); its value is  $5.5 \times 10^{-10} \text{ m}^2/\text{s}$ . The viscosity and the density of the solution were taken from data compiled by Weast (1977-1978). The bed void fractions for 3 × 3 mm and 6 × 6 mm glass cylinders were 0.349 and 0.362, and stagnant holdups were 0.153 and 0.12, respectively. The solid-liquid mass transfer measurements were made in the trickle, ripple, and pulse flow regimens. The liquid mass velocities were varied from 2.99 to 26.6  $\text{kg}/\text{m}^2\cdot\text{s}$  and gas mass velocities from 0.07 to 1.16  $\text{kg}/\text{m}^2\cdot\text{s}$ .

#### Data Sampling and Acquisition

The measuring apparatus for mass transfer and the data acquisition system are shown schematically in Figure 2. The DC voltage converted from an AC power supply unit was constant within an accuracy of 0.03% for a 10% change in AC voltage. A desired voltage between the electrodes was set and the resulting current was determined from the voltage drop across a 10 ohm standard resistor. The voltage signal was amplified and digitized by an AR 11 A/D converter and later processed in a DEC PDP 11/04 computer to get the data on mass transfer fluctuations. The potential drop between the electrodes varied within a maximum of 5% of the set value due to changes of liquid resistance when the liquid-rich parts (pulses) and the gas-rich parts passed the cell successively. However, this change in potential drop is negligible compared to the voltage range over which the limiting current plateau is attained. Thus, with the present measuring apparatus the limiting current could be reached both in and outside the pulses.

The column was first operated for at least 1 h in the pulse flow regime at high liquid rates to accomplish complete wetting of the packing. At the start of each experiment the limiting current plateau was determined by slowly increasing the voltage. Data sampling and acquisition in pulse flow were as follows: For a fixed liquid and gas rate a buffer of 500 data points was sampled consisting of more than one pulse in general. Then the buffer was scanned from the beginning to detect the start, the maximum, and the end of the first complete pulse in the buffer, taking care of the noise in the signal. The remaining data points in the buffer were discarded. The maximum value of the pulse is called the pulse mass transfer and the minimum value at the end of the pulse is called the base mass transfer, taken as representative of the part of the bed outside the pulses. The area under the curve from the start to the end of the pulse was integrated to give the average mass transfer. The procedure was repeated 100 times at each set point and statistical means for pulse, base, and average mass transfer were calculated. One experimental point took 2 h.

Under trickle and ripple flow conditions, the column was operated for about 30 min to reach steady state conditions. Then a buffer consisting of 1,000 data points was sampled in 5 to 10 min and averaged.

A direct comparison of the values of the limiting current on a current meter agreed well with the average computed value in trickle flow conditions, but a similar comparison was not possible in ripple flow conditions due to random fluctuations in the current.

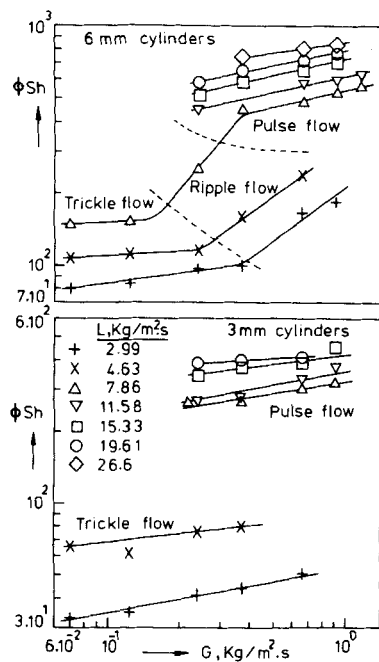


Figure 5. Experimental average mass transfer as a function of gas mass velocity for 6 mm and 3 mm cylinders.

## EXPERIMENTAL RESULTS AND DISCUSSION

The electrochemical technique measures the product of the local instantaneous mass transfer rate and the fractional surface wetting of the particle,  $\phi$ . Therefore all the mass transfer measurements are presented in terms of the product  $\phi Sh$ ,  $Sh$  being the Sherwood number. Various reports in the literature (e.g., Chou et al., 1979) indicate that nonuniform and incomplete surface wetting exists in trickle flow, while a uniform and complete wetting can be assumed under pulse flow conditions.

The experimental results for solid-liquid mass transfer in terms of  $\phi Sh$  are presented as a function of gas and liquid velocities in Figures 3 to 6. The pulse and base (outside the pulses) mass transfer coefficients in terms of  $\phi Sh$  increase with increasing liquid and gas mass velocities, as shown in Figures 3 and 4 for the packings of 6 mm and 3 mm cylinders, respectively. The increase in  $\phi Sh$  with  $L$  and  $G$  in pulse flow can be interpreted according to certain pulse properties first measured by Blok and Drinkenburg (1982) and supported by Rao and Drinkenburg (1983). The wetting of the particles as such may not be expected to contribute additionally to solid-liquid mass transfer after the inception of the pulses. Therefore, the increase of base and pulse mass transfer (Figures 3 and 4) may well be explained as follows:

- At a given liquid velocity, the interstitial liquid velocity increases with increasing gas velocity due to a decrease in liquid holdup.
- Interpretation of the residence time distribution measurements with the crossflow model shows that stagnant liquid holdup decreases with increasing pulse frequency and with decreasing total liquid holdup (Blok, 1981). The increased mobility of the liquid induces more turbulence, especially at the packing junctions. This phenomenon may also be true for base mass transfer but at a different level of turbulence.
- The liquid in the pulse is accelerated by the higher pulse velocity, which is approximate an order of magnitude higher than the interstitial velocity of the liquid.

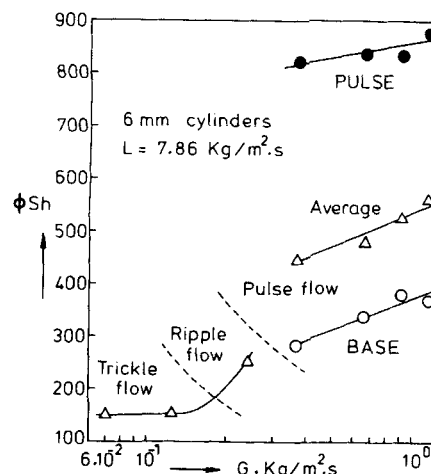


Figure 6. Typical comparison of experimental mass transfer in trickle, ripple, and pulse flow regimes.

- Blok et al (1983) observed that the transition flow occurs at a constant critical liquid velocity,  $V_{Lt}$ , and the pulse frequency,  $f_p$ , is given by

$$f_p \propto (V_L - V_{Lt}) \quad (2)$$

A small increase in  $V_{Lt}$  with liquid velocity at the transition to pulse flow regime was observed (Rao and Drinkenburg, 1983), which obviously increases the base mass transfer with increasing liquid rate.

The time-averaged solid-liquid mass transfer coefficients in terms of  $\phi Sh$  in trickle, ripple, and pulse flow are shown in Figure 5 for 6 mm and 3 mm cylinders.  $\phi Sh$  increases with both gas and liquid mass velocities in all the flow regimens. The dotted lines in Figures 5 and 6 for 6 mm cylinders delineate approximately the data in the respective flow regimes. As can be seen from Figure 5 and 6 for 6 mm cylinders, at a constant  $L$ ,  $\phi Sh$  increases rather slowly with increasing  $G$  in trickle flow. Further increase in  $G$  causes rippling, probably creating turbulence in the liquid film, and the mass transfer begins to increase significantly. The increase is accompanied by fluctuations in mass transfer. The fluctuations become larger with increasing  $G$ . In this range of  $G$  no such fluctuations in mass transfer occurred for 3 mm cylinders. The increase in solid-liquid mass transfer with  $G$  in trickle flow and for the transition (ripple, incipient pulsing) was also reported for Sylvester and Pitayagulsarn (1975) and Ruether et al. (1980).

$\phi Sh$  in trickle flow (Figure 5) increases with  $L$  due to increasing interstitial velocity of the liquid and fractional surface wetting,  $\phi$ , of the particles. The increase in  $\phi Sh$  with  $G$  is small for high liquid mass velocity  $L$ , but for low liquid mass velocities, the dependence of  $\phi Sh$  on  $G$  can be strong. Specchia et al. (1978) also noticed an increase in  $\phi Sh$  with increasing  $G$  in trickle flow. Satterfield et al. (1978) reported a maximum of 10% change in  $\phi Sh$  with  $G$  in the trickle-flow regime. Contrary to the above, Hirose et al. (1976) found no effect of  $G$  on  $\phi Sh$  in trickle flow.

The mass transfer coefficients  $\phi k_s$  for 3 mm cylinder are smaller than for 6 mm cylinders at  $L = 2.99 \text{ kg/m}^2\text{s}$  (Figure 5). It should be noted that a decrease in  $\phi k_s$  is predicted at sufficiently lower liquid Reynolds numbers (Carberry, 1960) and the enhancement of  $\phi k_s$  is expected to be smaller for decreasing particle size (Goto et al., 1975).

Figure 6 shows a typical comparison of  $\phi Sh$  between pulse, base, and average mass transfer in pulse and  $\phi Sh$  values in trickle flow and ripple flow at  $L = 7.86 \text{ kg/m}^2\text{s}$  for 6 mm cylinders. The effect of gas rate is marked in the ripple flow regime. Having attained a certain level of turbulence and almost complete wetting

of the particles at the inception of pulses, the base mass transfer continues to increase with increasing  $G$  but less steeply than in ripple flow. The curve for trickle-ripple-base might well be continuous. The turbulence in the pulse is very high, causing a significant increase in pulse mass transfer that is about 2.5 times greater than the base mass transfer for 6 mm cylinders. Also, as can be seen from Figure 6, mass transfer for base, average, and pulse at  $G = 0.37 \text{ kg/m}^2\text{-s}$  increases by about 2, 3, and 5.5 times, respectively, compared to  $\phi Sh$  for trickle flow.

It can be noticed from Figure 5 that the mass transfer in terms of  $\phi k_s$  increases with decreasing particle diameter. It is interesting to note that on the average  $\phi k_s$  for pulses increases by about 40% for 3 mm cylinders over 6 mm cylinders, whereas the increase in  $\phi k_s$  for 3 mm cylinders in pulse flow is about 25% higher than for 6 mm cylinders. The relative lower enhancement of mass transfer for smaller particle size in the low interaction regime (parts outside the pulse) was also noticed by Goto et al. (1975) in trickle flow for smaller packings ( $\leq 2.4 \text{ mm}$ ). However, the operating conditions were different in the two situations. While complete wetting of the particles can be assumed in pulse flow, this is not so in the trickle flow regime. This leaves us to believe that the relative decrease of enhancement for smaller packings in low interaction regions is due to a relative decrease of turbulence or a relative increase of stagnant liquid holdup at the packing junctions. For smaller particles the stagnant liquid holdup at the packing junctions occupies a relatively large fraction of the particle surface, eventually leading to overlapping.

## CORRELATION OF RESULTS

Table 1 summarizes the relevant earlier studies on solid-liquid mass transfer.

### Trickle Flow

The mass transfer data in ripple flow and the data for 3 mm cylinders at  $L = 2.99 \text{ kg/m}^2\text{-s}$  were compared with the earlier correlations. The Specchia et al. (1978) and Satterfield et al. (1978) correlations at  $G = 0$  for incomplete fractional wetting agree with our data with root mean square deviations of about 14%. The Goto et al. (1975) graphical correlation predicts a maximal 25% higher value at the lowest gas rate ( $G = 0.07 \text{ kg/m}^2\text{-s}$ ) for both packings. Our results when compared with the Van Krevelen and Kerkels (1948) correlation for filmlike flow did not agree at all, the correlation predicting very high values.

The correlation of Ruether et al. (1980) for trickle flow, taking an average porosity of 0.615 for 6.35 mm berl saddles, can be written as

$$\phi Sh/Sc^{1/3} = 0.133 (Re_L^*)^{0.777} \quad (3)$$

The liquid holdups required to calculate  $Re_L^*$  were obtained using Specchia and Baldi's (1977) equation in the low interaction regime as given by Eq. 4:

$$\beta_d = 3.86 Re_L^{0.545} (Ga^*)^{-0.42} (a_s d_p / \epsilon)^{0.65} \quad (4)$$

Our experimental mass transfer data agree with the values calculated by Eq. 3 with a root mean square relative deviation of 11%. However, the values from Eq. 4 were consistently lower, with a maximum deviation of 16%.

The analysis of the present data and the data of earlier investigators indicate that the effect of gas rate on solid-liquid mass transfer rates is significant for  $G > 0.01 \text{ kg/m}^2\text{-s}$ , and none of the existent correlations is capable of correlating the data with good accuracy. With the aim to improve the correlating accuracy for the mass transfer data in trickle flow for  $G > 0.01 \text{ kg/m}^2\text{-s}$ , an equation containing Sherwood and Schmidt numbers as proposed by Satterfield et al. and a modified liquid Reynolds number  $Re_L'$

$= Ld_p'/h_L\mu_L$ ) is proposed, Eq. 5. The liquid holdup,  $h_L$ , based on column volume is expected to take into account the effect of accompanying gas flow on solid-liquid mass transfer. The dynamic liquid holdups are calculated by Eq. 4 and the stagnant liquid holdups,  $\beta_s$ , from the relation proposed by Mersmann as reported by Hofmann (1978).

Our experimental data, fitted by linear least-squares regression, give the following equation:

$$\phi Sh'/Sc^{1/3} = 0.24 (Re_L')^{0.75} \quad (5)$$

The root mean square relative deviation with our data is 6.5% (Figure 7). Also the data of Ruether et al. for 6.35 mm Berl saddles, recalculated from their relation, and those from Chou et al. (1979) at  $u_G = 0.286 \text{ m/s}$  for 7.8 mm spheres and the data of Sylvester and Pitayagulsarn (1975) for 3.17 mm cylindrical pellets are compared with proposed Eq. 5 in Figure 7. The pressure drops required to calculate dynamic liquid holdups from Eq. 4 were obtained from the correlation proposed by Rao et al. (1983) in trickle flow given by Eq. 6.

$$(-\Delta P/H) = 0.239 \frac{L^{0.4} G^{0.95} (1 - \epsilon)^{1.5}}{d_e^{1.69} \epsilon^{2.2}} \quad (6)$$

As can be seen from Figure 7, the data of Ruether et al. and Chou et al. agree with the proposed correlation, while those of Sylvester fall below the line within a 15% error bound.

### Pulse Flow

Our results for the average mass transfer agree reasonably well with the correlation proposed by Chou et al. (1979) based on their transfer data by the electrochemical technique from a single sphere ( $d_p = 7.8 \text{ mm}$ ). The results spread with a root mean square relative deviation of 7.3%. When our data for pulse, base, and average mass transfer are fitted by nonlinear least-squares regression to the same type of equation as theirs, the following relations are obtained:

Pulse mass transfer:

$$\epsilon \phi Sh''/Sc^{1/3} = 2.4 Re_L^{0.34} Re_G^{0.18} \quad (7)$$

Base mass transfer:

$$\epsilon \phi Sh''/Sc^{1/3} = 0.31 Re_L^{0.44} Re_G^{0.323} \quad (8)$$

Average mass transfer:

$$\epsilon \phi Sh''/Sc^{1/3} = 0.77 Re_L^{0.45} Re_G^{0.223} \quad (9)$$

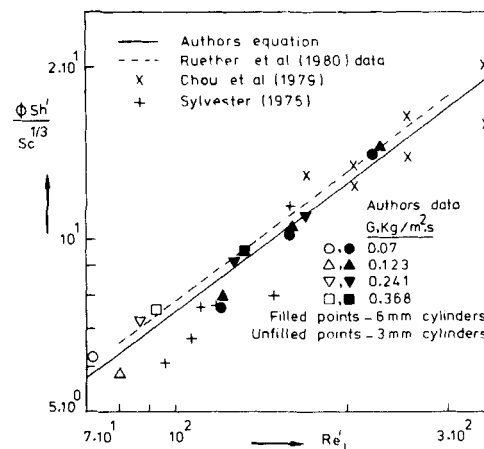


Figure 7. Comparison of solid-liquid mass transfer data in trickle flow with authors correlation, Eq. 5.

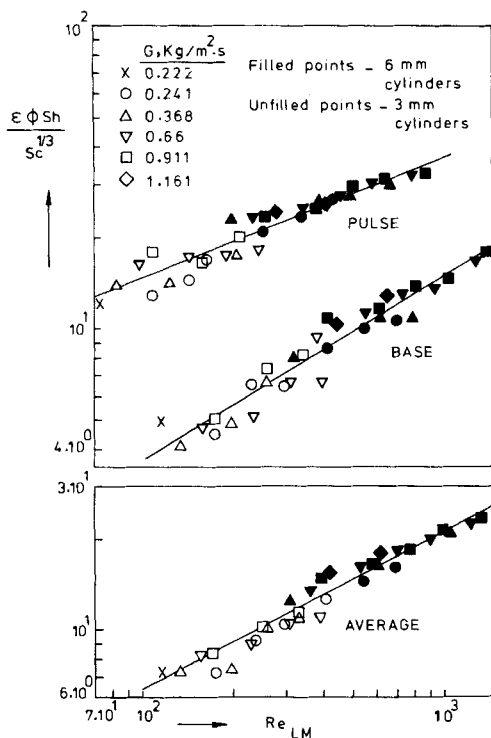


Figure 8. Correlations for pulse, base, and average solid-liquid mass transfer, Eqs. 17, 18, 19.

The root mean square relative deviations for the above equations are 6.7, 10.5, and 5.5%, respectively.

Comparison of the experimental data of mass transfer with the equation of Ruether et al. (1980) requires the liquid holdups. The holdup equations of Blok and Drinkenburg (1982) were used to calculate the pulse, base, and average liquid holdups in pulse flow:

Pulse liquid holdup:

$$\beta_p = 0.058(a_s/U_G)^{0.29} \quad (10)$$

Base liquid holdup:

$$\beta_p = 0.036(a_s/U_G)^{0.29} \quad (11)$$

Average liquid holdup:

$$\beta = 0.048(a_s/U_G)^{0.265} \quad (12)$$

Although these equations were based on Raschig rings data, the applicability of these equations was checked for other types of packings such as spheres (Rao and Drinkenburg, 1983).

The equation of Ruether et al. (1980), taking an average porosity of 0.615 for Berl saddles, can be written as

$$\phi Sh^*/Sc^{1/3} = 1.11(Re_L^*)^{0.416} \quad (13)$$

The calculated values for Eq. 13 were consistently lower, deviating by about 30% for 6 mm cylinders, although comparison was better for 3 mm cylinders, whereas the Specchia et al. (1978) correlation did not agree satisfactorily with our average mass transfer results. The data of Sylvester and Pitayagulsarn (1975) were lower than our results and the same may be expected with the data of Satterfield et al. (1978) at  $L = 5 \text{ kg/m}^2\text{s}$  due to their reported agreement of their data with those of Sylvester and Pitayagulsarn.

The time-averaged mass transfer rates measured by using a single active particle (present study and Chou et al., 1979) were usually higher than those measured by the dissolution method. This

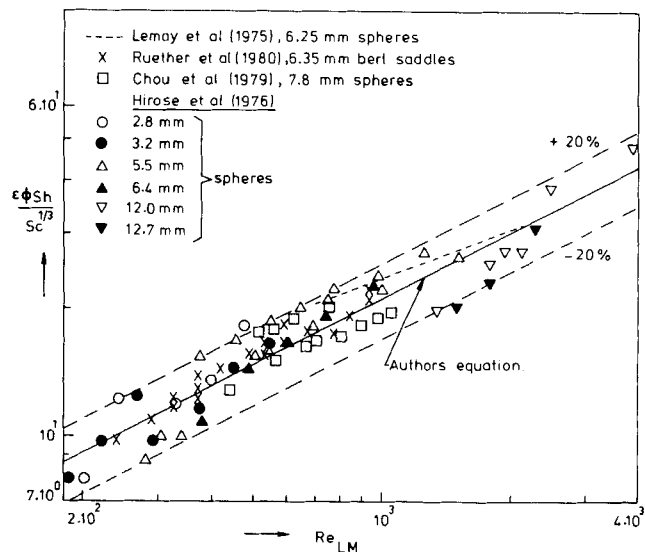


Figure 9. Comparison of the average solid-liquid mass transfer data in pulse and dispersed bubble flow reported in the literature with the authors' correlation, Eq. 19.

difference may be due to several factors, as mentioned by Chou et al. (1979).

With the aim of improving the correlation of our data as well as the previous data, various forms of correlating equations were tried. Of these, the form given below was found the best.

$$\epsilon \phi Sh / Sc^{1/3} = A Re_{LM}^B \quad (14)$$

with

$$Sh = k_s d_e / D \quad (15)$$

$$Re_{LM} = L d_e / h_i \mu_L \quad (16)$$

where  $d_e = 6(1 - \epsilon)/a_s$  is the effective particle diameter.

Our mass transfer data for pulse, base, and average were fitted to the form of Eq. 14 by nonlinear least-squares regression to give the following equations:

Pulse mass transfer:

$$\epsilon \phi Sh / Sc^{1/3} = 2.38 Re_{LM}^{0.4} \quad (17)$$

Base mass transfer:

$$\epsilon \phi Sh / Sc^{1/3} = 0.29 Re_{LM}^{0.56} \quad (18)$$

Average mass transfer:

$$\epsilon \phi Sh / Sc^{1/3} = 0.58 Re_{LM}^{0.519} \quad (19)$$

Our data are compared with the equations in Figure 8. The root mean square relative deviations are 8.9, 11.2, and 8.2%, respectively. The liquid holdups are calculated with the help of Eqs. 10–12. No significant deviations were noticed when the holdup equations of Rao et al. (1983) and Specchia and Baldi (1977) were employed to test the average mass transfer data. The average mass transfer correlation given by Eq. 19 is compared in Figure 9 with the data reported by earlier investigators in pulse and dispersed bubble flow. The data reported by Ruether et al. (1980) in dispersed bubble flow were recalculated using the Rao et al. (1983) correlation for total liquid holdup:

$$\beta = 0.045 a_s^{1/3} (Re_L / Re_G)^{1/5} \quad (20)$$

As can be seen from Figure 9, the present correlation given by Eq. 19 is able to correlate all the data within  $\pm 20\%$  error bounds for the

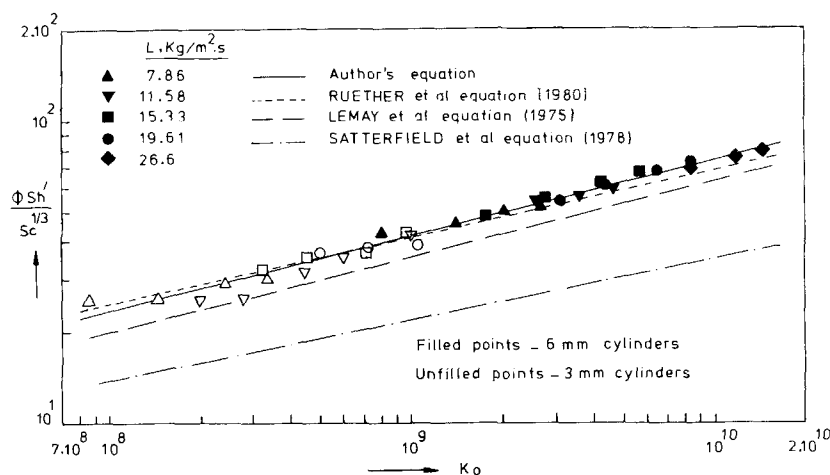


Figure 10. Comparison of authors' average mass transfer data and correlation with earlier correlations in terms of Kolmogoroff number.

packings of different shapes such as spheres, cylinders, and Berl saddles. The liquid mass velocity  $L$  was varied from 7.5 to 95  $\text{kg/m}^2\text{s}$  and the gas mass velocity was varied from 0.08 to 2.4  $\text{kg/m}^2\text{s}$ . The modified Reynolds number  $Re_{LM}$  was varied from 184 to 3930.

#### CORRELATION USING THE ENERGY DISSIPATION

Lemay et al. (1975), following the approach of Calderbank and Moo-Young (1961), correlated the mass transfer coefficients in packed beds under pulsing conditions by using the energy dissipation as given by Eq. 21. This equation assumes no explicit dependence of  $k_s$  on particle diameter but only implicitly through energy dissipation.

$$\phi k_s Sc^{2/3} = 0.20 (E'_L \mu_L / \rho_L)^{0.25} \quad (21)$$

Satterfield et al. (1978) correlated their mass transfer rates by energy dissipation in the form of Kolmogoroff numbers, in which the effect of particle diameter can be explicitly taken. Their results at  $L = 4.9 \text{ kg/m}^2\text{s}$  were correlated by

$$\phi Sh' / Sc^{1/3} = 0.334 Ko^{0.202} \quad (22)$$

where

$$\phi Ko = E'_L (d_p)^4 \rho_L^3 / \mu_L^3 \quad (23)$$

Their results at  $L = 25 \text{ kg/m}^2\text{s}$  were found to agree with the Lemay et al. correlation, which can be written in terms of the Kolmogoroff number, Eq. 24:

$$\phi Sh' / Sc^{1/3} = 0.20 Ko^{0.25} \quad (24)$$

Ruether et al. (1980) proposed Eq. 25 based on their data for Berl saddles in pulse flow and dispersed bubble flow:

$$\phi Sh' / Sc^{1/3} = 0.43 Ko^{0.22} \quad (25)$$

The values of the Kolmogoroff numbers are very high, varying approximately between  $10^8$  and  $10^{10}$  for pulse flow. It should be noted that a small change in the exponent of  $Ko$  causes considerable difference in the constant.

Our average mass transfer data for 3 mm and 6 mm cylinders were also correlated using the Kolmogoroff number to give Eq. 26:

$$\phi Sh' / Sc^{1/3} = 0.23 Ko^{0.25} \quad (26)$$

Our correlation and data are compared with the earlier correlations in Figure 10. The root mean square relative deviation of the data with the proposed correlation (Eq. 26) is 5%. As can be seen from Figure 10, among all other earlier correlations, the Ruether et al. correlation agrees well with our data with a root mean relative deviation of 7%. The correlation of Lemay et al. falls about 15% below our correlation. The Satterfield et al. correlation underestimates our results as much as 50% on the average. Agreement of our data for 3 mm and 6 mm cylinders with the exponent of 0.25 to the Kolmogoroff number indicates no explicit effect of packing diameter on  $k_s$ , in contrast with the findings of Ruether et al. and Satterfield et al. However, it should be noted that the correlation of Ruether et al. was based on one-third of their experimental data taken in pulse flow and two-thirds of their data taken in dispersed bubble flow.

#### COMPARISON BETWEEN PULSES AND DISPERSED BUBBLE FLOW

Pulses may be assumed to be parts of the bed already in dispersed bubble flow. If the pulse mass transfer can be correlated by Kolmogoroff numbers representing the pulse, then the resulting correlation may be expected to provide more information about the nature of the pulse and probably the influence of the particle diameter in dispersed bubble flow.

Rao and Drinkenburg (1984) proposed a model to calculate pressure drop in pulse flow. This model was verified with extended experimental data for Raschig rings and spheres in various column diameters. Agreement was highly satisfactory. Utilizing the same experimental data and the model, the fractional pressures drops (in total pressure) due to pulses,  $x_p$ , were calculated and correlated by nonlinear least-squares regression to give the following equation:

$$x_p = 7.66 U_L^{0.65} / \epsilon^{0.4} \quad (27)$$

Assuming Eq. 27 will hold for 3 mm and 6 mm cylinders, the pressure drop per pulse was calculated from the knowledge of two-phase pressure drop, pulse frequency, and pulse velocity. Assume moreover that the pulse velocity was not very different from 1 m/s and that the effective average pulse height was 5 cm. The assumptions may be justified based on the pulse height and pulse velocity measurements of Blok and Drinkenburg (1982) and Rao and Drinkenburg (1983). Then Kolmogoroff numbers for pulses were calculated, also taking the pulse holdups into consideration.



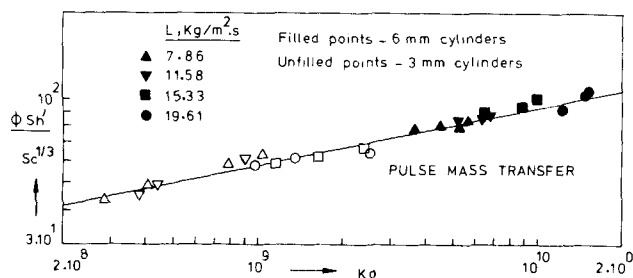


Figure 11. Correlation for pulse mass transfer.

Performing a nonlinear least-square fit on the mass transfer measurements in the pulses proper and the corresponding Kolmogoroff numbers resulted in Eq. 28 for pulse mass transfer, which is compared with the data in Figure 11.

$$\phi Sh' Sc^{1/3} = 0.71 Ko^{0.21} \quad (28)$$

The root mean square relative deviation from the data is 4.6%. Comparison of Eqs. 28 and 25 shows reasonable agreement of the exponent on  $Ko$ , although the constants in the equations are different. Equation 25 represents the data of Ruether et al., mostly in dispersed bubble flow, and Eq. 28 represents our pulse mass transfer data.

The constants in Eqs. 25 and 28 differ due to the fact that  $Ko$  numbers in Eq. 28 were based on the average superficial liquid velocity in the column instead of superficial liquid velocity in the pulses. For good comparison an estimate of the superficial liquid velocity in the pulses was obtained as follows: From the knowledge of pressure drop per pulse and a pulse height of 5 cm, the pressure drop per unit height of pulse was calculated. The liquid rate required (in dispersed bubble flow) to attain the pressure drop equal to the pressure drop per unit height of the pulse was calculated from the pressure drop correlation given by Rao et al. (1983) for dispersed bubble flow:

$$(-\Delta P/H) = 0.096 \frac{L^{1.05} G^{0.4} (1-\epsilon)^{1.5}}{d_e^{1.54} \epsilon^{2.2}} \quad (29)$$

The Kolmogoroff numbers were then calculated using the liquid rates obtained from Eq. 29 and the pressure drops per unit height of the pulse. Pulse mass transfer data are plotted against the simulated Kolmogoroff numbers (in dispersed bubble flow) in Figure 12 and are compared with the Ruether et al. correlation. The data now agree satisfactorily with the Ruether et al. correlation, Eq. 25, with a root mean square relative deviation of 9.3%.

The satisfactory agreement of our pulse mass transfer data with the correlation applicable to dispersed bubble flow indicates that the  $k_s$  in the pulses closely corresponds to  $k_s$  in dispersed bubble flow. This finding, together from the knowledge of certain pulse properties and the bubble dispersion in the pulses observed by high-speed photography, supports the idea that the hydrodynamics inside the pulses are similar to those in dispersed bubble flow and thus that pulses may be considered to be parts of the bed already in dispersed bubble flow.

#### ACKNOWLEDGMENT

The authors wish to thank Han Kalsbeek for making available some of his computer programs and Laurens Bosgra for taking care of the electronics.

#### NOTATION

$A$  = constant  
 $a$  = effective external solid surface area for mass transfer

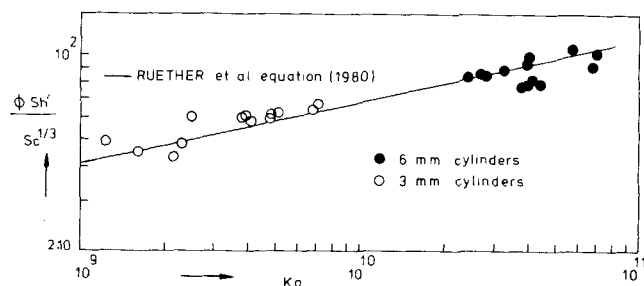


Figure 12. Authors' pulse mass transfer data vs. simulated Kolmogoroff numbers in dispersed bubble flow and comparison with Ruether et al. (1980) correlation, Eq. 25.

$a_s$  = external surface area of the packing per unit column volume,  $m^2/m^3$   
 $B$  = constant  
 $c$  = concentration at saturation,  $mol/m^3$   
 $D$  = molecular diffusivity,  $m^2/s$   
 $d_p$  = particle diameter,  $m$   
 $d_p^*$  = equivalent particle diameter of a sphere having the same surface area as the particle in question,  $m$   
 $d_e$  = effective particle diameter,  $= 6(1-\epsilon)/a_s$ ,  $m$   
 $E_L$  = energy dissipated by liquid phase per unit mass of external liquid holdup,  $= (-\Delta P/H)U_L/h_t\rho_L$ ,  $m^2/s^3$   
 $f_p$  = pulse frequency,  $1/s$   
 $G$  = superficial gas mass velocity,  $kg/m^2\cdot s$   
 $Ga^*$  = modified Galileo number,  $= d_p^3\rho_L(\rho_L G + \Delta P/H)/\mu_L^2$   
 $H$  = height,  $m$   
 $h_t$  = external liquid holdup, volume of the liquid per unit column volume,  $= \beta_s + \beta_d$   
 $j_D$  = mass transfer factor,  $= (ak_s/a_s U_L)Sc^{2/3}$   
 $K_{LS}$  = overall mass transfer coefficient in liquid,  $m/s$   
 $k_s$  = solid-liquid mass transfer coefficient,  $m/s$   
 $Ko$  = liquid phase Kolmogoroff number,  $= E_L(d_p^*)^4\rho_L^3/\mu_L^3$   
 $L$  = superficial liquid mass velocity,  $kg/m^2\cdot s$   
 $(-\Delta P/H)_{LG}$  = two-phase pressure drop per unit height of the column,  $N/m^3$   
 $r$  = reaction rate,  $mol/m^3\cdot s$   
 $Re_G$  = gas phase Reynolds number,  $= Gd_p/\mu_G$   
 $Re_L$  = liquid phase Reynolds number,  $= Ld_p/\mu_L$   
 $Re_L'$  = modified liquid phase Reynolds number,  $= L/h_t a_s \mu_L$   
 $Re_L''$  = modified liquid phase Reynolds number,  $= Ld_p'/h_t \mu_L$   
 $Re_L'''$  = modified liquid phase Reynolds number,  $= L/a_s \mu_L$   
 $Re_L''''$  = modified liquid phase Reynolds number,  $= Ld_p'/\mu_L$   
 $Re_{LM}$  = modified liquid phase Reynolds number,  $= Ld_e/h_t \mu_L$   
 $Sc$  = Schmidt number of liquid,  $= \mu/\rho D$   
 $Sh$  = Sherwood number of liquid,  $= k_s d_e/D$   
 $Sh'$  = Sherwood number of liquid,  $= k_s d_p'/D$   
 $Sh''$  = Sherwood number of liquid,  $= k_s d_p/D$   
 $Sh^*$  = Sherwood number of liquid,  $= k_s/a_s D$   
 $U_L$  = superficial velocity of liquid,  $m/s$   
 $U_G$  = superficial velocity of gas,  $m/s$   
 $V_L, V_{Lt}$  = real (interstitial) velocity of liquid,  $m/s$   
 $We$  = Weber number,  $= U_L^2 \rho_L d_p / \sigma_L h_t^2$   
 $x_p$  = fraction in total pressure drop, contributed by pulsing part in the column

## Greek Letters

$\epsilon$	= void fraction of the bed
$\mu, \mu_L$	= viscosity of liquid, kg/m·s
$\mu_G$	= viscosity of gas, kg/m·s
$\rho, \rho_L$	= density of liquid, kg/m <sup>3</sup>
$\rho_G$	= density of gas, kg/m <sup>3</sup>
$\sigma_L$	= surface tension of the liquid phase, N/m
$\phi$	= fractional particle wetting with active liquid, = $a/a_s$
$\beta$	= external liquid holdup, volume of the liquid per unit void volume in the bed
$\beta_d$	= liquid holdup, dynamic
$\beta_p$	= liquid holdup, pulse
$\beta_b$	= liquid holdup, base
$\beta_s$	= liquid holdup, stagnant

## LITERATURE CITED

- Blok, J. R., "Pulsing Flow in Trickle Bed Columns," Ph.D. Thesis, Rijksuniversiteit Groningen (1981).
- Blok, J. R., and A. A. H. Drinkenburg, "Hydrodynamic Properties of Pulses in Two-Phase Downflow Operated Packed Columns," *Chem. Eng. J.*, **25**, 89 (1982).
- Blok, J. R., J. Varkevisser, and A. A. H. Drinkenburg, "Transition to Pulsing Flow, Holdup and Pressure Drop in Packed Columns with Cocurrent Gas-Liquid Downflow," *Chem. Eng. Sci.*, **38**, 687 (1983).
- Calderbank, P. H., and M. B. Moo-Young, "The Continuous Phase Heat and Mass Transfer Properties of Dispersions," *Chem. Eng. Sci.*, **16**, 39 (1961).
- Carberry, J. J., "A Boundary-Layer Model of Fluid-Particle Mass Transfer in Fixed Beds," *AIChE J.*, **6**, 460 (1960).
- Chou, T. S., F. L. Worley, Jr., and D. Luss, "Local Particle-Liquid Phase Mass Transfer, Fluctuations in Mixed-Phase Cocurrent Downflow Through a Fixed Bed in the Pulsing Regime," *Ind. Eng. Chem. Fund.*, **18**, 279 (1979).
- Delaunay, G., et al., "Electrochemical Study of Liquid-Solid Mass Transfer in Packed Beds with Upward Cocurrent Gas-Liquid Flow," *Ind. Eng. Chem. Process Des. Dev.*, **19**, 514 (1980).
- , "Electrochemical Determination of Liquid-Solid Mass Transfer in a Fixed Bed Irrigated Gas-Liquid Reactor with Downward Co-current Flow," *Intern. Chem. Eng.*, **22**, 244 (1982).
- Goto, S., J. Levec, and J. M. Smith, "Mass Transfer in Packed Beds with Two-Phase Flow," *Ind. Eng. Chem. Process Des. Dev.*, **14**, 473 (1975).
- Hiraoka, S., et al., "Measurement of Diffusivities of Ferricyanide and Ferrocyanide Ions in Dilute Solution with KOH Supporting Electrolyte," *J. Chem. Eng. Japan*, **145**, 345 (1981).
- Hirose, T., Y. Mori, and Y. Sato, "Liquid-to-Particle Mass Transfer in Fixed Bed Reactor with Cocurrent Gas-Liquid Downflow," *J. Chem. Eng. Japan*, **9**, 220 (1976).
- Hofmann, H. P., "Multiphase Catalytic Packed-Bed Reactors," *Catal. Rev. Sci. Eng.*, **17**, 71 (1978).
- Krevelen, D. W. van, and J. T. C. Krekels, "Rate of Dissolution of Solid-Substances. I. Rate of Mass Transfer in Granular Beds (Physical Dissolution)," *Rec. Trav. Chim. Pays-Bas*, **67**, 512 (1948).
- Lemay, Y., G. Pineault, and A. Ruether, "Particle-Liquid Mass Transfer in a Three-Phase Fixed Bed Reactor with Cocurrent Flow in the Pulsing Regime," *Ind. Eng. Chem. Process Des. Dev.*, **14**, 280 (1975).
- Rao, V. G., M. S. Ananth, and Y. B. G. Varma, "Hydrodynamics of Two-Phase Cocurrent Downflow Through Packed Beds. II. Experiment and Correlations," *AIChE J.*, **29**, 473 (1983).
- Rao, V. G., and A. A. H. Drinkenburg, "Pressure Drop and Hydrodynamic Properties of Pulses in Two-Phase Gas-Liquid Downflow Through Packed Columns," *Can. J. Chem. Eng.*, **61**, 158 (1983).
- , "A Model for Pressure Drop Based on Liquid Holdup Data in Two-Phase Gas-Liquid Downflow Through Packed Columns," *AIChE J.*, **31**(6) (June, 1985).
- Ruether, J. A., Ching-Shi Yang, and W. Hayduk, "Particle Mass Transfer During Cocurrent Downward Gas-Liquid Flow in Packed Beds," *Ind. Eng. Chem. Process Des. Dev.*, **19**, 103 (1980).
- Satterfield, C. N., "Trickle-Bed Reactors," *AIChE J.*, **21**, 209 (1975).
- Satterfield, C. N., N. W. van Eek, and G. S. Bliss, "Liquid-Solid Mass Transfer in Packed Beds with Downward Concurrent Gas-Liquid Flow," *AIChE J.*, **24**, 709 (1978).
- Specchia, V., and G. Baldi, "Pressure Drop and Liquid Holdup for Two-Phase Concurrent Flow in Packed Beds," *Chem. Eng. Sci.*, **32**, 515 (1977).
- Specchia, V., G. Baldi, and A. Gianetto, "Solid-Liquid Mass Transfer in Concurrent Two-Phase Flow Through Packed Beds," *Ind. Eng. Chem. Process Des. Dev.*, **17**, 362 (1978).
- Sylvester, N. D. and P. Pitayagulsarn, "Mass Transfer for Two-Phase Cocurrent Downflow in a Packed Bed," *Ind. Eng. Chem. Process Des. Dev.*, **14**, 421 (1975); correction, *ibid.*, **15**, 360 (1976).
- Weast, C. R., *Handbook of Chemistry and Physics*, CRC Press (1977–78).

Manuscript received May 26, 1983; revision received July 26 and accepted July 30, 1984.